Operating Modes and Cooling Capabilities of the 3-Stage ADR Developed for the Soft-X-ray Spectrometer Instrument on Astro-H

Peter J Shirron[1], Mark O Kimball[1], Bryan L James[1], Theo Muench[1], Michael J DiPirro[1], Richard V Letmate[2], Michael A Sampson[3], Tom G Bialas[1], Gary A Sneiderman[1], Frederick S Porter[1], Richard L Kelley[1]

[1]*NASA/Goddard Space Flight Center, Greenbelt, MD 20771 USA*
[2]*Bastion Technologies, 7515 Mission Drive, Suite 300 Lanham, MD 20706 USA*
[3]*SGT Inc., 7701 Greenbelt Road, Suite 400 Greenbelt, MD 20770 USA*

ABSTRACT

A 3-stage adiabatic demagnetization refrigerator (ADR)[1] is used on the Soft X-ray Spectrometer instrument[2] on Astro-H[3] to cool a 6x6 array of x-ray microcalorimeters to 50 mK. The ADR is supported by a cryogenic system[4] consisting of a superfluid helium tank, a 4.5 K Joule-Thomson (JT) cryocooler, and additional 2-stage Stirling cryocoolers that pre-cool the JT cooler and cool radiation shields within the cryostat. The ADR is configured so that it can use either the liquid helium or the JT cryocooler as its heat sink, giving the instrument an unusual degree of tolerance for component failures or degradation in the cryogenic system. The flight detector assembly, ADR and dewar were integrated into the flight dewar in early 2014, and have since been extensively characterized and calibrated. This paper summarizes the operation and performance of the ADR in all of its operating modes.

INTRODUCTION

The Soft X-ray Spectrometer instrument[2] on Astro-H will contain the most sensitive x-ray microcalorimeters ever launched into orbit. Each pixel in the 6x6 array has an intrinsic energy resolution of better than 5 eV (at 6 keV) and sensitivity to x-rays in the 0.2 to 13 keV energy band[5]. This sensitivity is achieved in part by cooling the array to very low temperature, 50 mK.

The SXS instrument draws on significant heritage from the X-Ray Spectrometer instrument[6] that was part of the instrument suite on Suzaku[7] (formerly Astro-E2). In particular, XRS used an ADR for detector cooling, and the ADR used a small superfluid helium tank as its heat sink. But unlike XRS, SXS is also designed to enable redundant operation of the ADR using a 4.5 K Joule-Thomson cryocooler[8] as a heat sink. The design philosophy is as follows. When liquid helium is present, the JT cryocooler acts as a shield for the helium tank in order to reduce the parasitic heat, enabling SXS to meet its three-year lifetime requirement[9]. After the liquid is depleted, the JT cryocooler acts as a heat sink for the ADR, which changes its operating mode to begin cooling both the helium tank and the detectors.

The SXS instrument is designed to meet the same top-level requirements in both cryogen and cryogen-free modes. These requirements stipulate a minimum detector performance (better than 7 eV resolution at 6 keV, and sensitivity over the energy range from 0.2 to 13 keV), and an observing efficiency of >90%. The latter refers to the percentage of time that the detectors are operational at 50 mK at the required energy resolution, and thus sets a limit for the duration of overhead operations such as ADR recycling, recovery of temperature stability after the recycle, and target acquisition.

The ADR's functional requirements are summarized in Table 1. They include specifications for detector temperature and stability, duty cycle, and heat output to the heat sinks. There is also a requirement for stability in the temperature of the detector housing, the structure that physically surrounds and supports the detector array. The heat leak into the detector array, through the Kevlar suspension and readout wires, depends only on the temperature of the housing. Fluctuations in the heat leak can cause time varying thermal gradients within the array, which can cause changes in detector gain, and uncertainty in the apparent energy of incoming x-rays. To limit the effect, the housing must be stable over times scales shorter than 10 minutes. (On longer time scales, the gain can be tracked using the response of a calibration pixel which observes x-rays from an Fe-55 source.) In cryogen mode, the housing is inherently stable due to the high heat capacity and thermal conductivity of superfluid helium. In cryogen-free mode, the ADR actively controls the detector housing temperature.

Table 1. Operating requirements for the SXS ADR in cryogen and cryogen-free modes.

	Cryogen mode	*Cryogen-free mode*
Detector temperature	50 mK	50 mK
Detector temperature stability	<2 μK rms	<2 μK rms
Detector heat load	0.25 μW (He tank at 1.3 K)	0.47 μW (He tank at 1.8 K)
Detector housing temperature		<1.8 K
Detector housing stability	<1 mK p-p over time scales of 0.2 sec to 10 minutes	<1 mK p-p over time scales of 0.2 sec to 10 minutes
Duty cycle	>90%	>90%
Heat rejection (time average)	<0.2 mW at 1.3 K	
Heat rejection (peak)		<30 mW at 4.5 K

The SXS ADR, consisting of three stages (S1-S3) and four heat switches (HS1-HS4), is arranged within the cryogenic system as shown in Figure 1. A 3D CAD model is shown in Figure 2. Details have been reported on previously for the design and optimization of the ADR[1,10,11,12], its salt pills[11], heat switches[13], magnets and shields[14], mechanical suspensions[14], and the cryogenic system[4] that supports its operation. Basic design and operating parameters are provided in Table 2 for reference.

Table 2. Design parameters of the SXS 3-stage ADR

	Stage 1	*Stage 2*	*Stage 3*
Magnetocaloric material	270 g CPA	147 g GLF	147 g GLF
Peak (average) magnetic field (T)	2	3	3
Maximum magnet current (amps)	2	2	2
Demagnetization temperature (K)	0.8	~1.5	4.5
Nominal operating temperature (K)	0.05	0.5	~1
Heat switch type	Gas-gap	Gas-gap	Gas-gap (2x)

The materials used in the salt pills, chrome potassium alum (CPA) or gadolinium lithium fluoride (GLF)[15], were chosen for their superior magnetocaloric properties in the temperature ranges over which they are used[16]. The refrigerant masses, magnetic fields and demagnetization temperature were chosen so that Stage 1 would achieve a cooling capacity, assuming 70% heat absorption efficiency, that accommodated the expected heat load (of 0.65 μW; see Table 3) for a 24-hour hold time, plus 100% margin. That requires a cooling capacity of at least 0.160 J. As designed, Stage 1 has a theoretical cooling capacity of 0.165 J at 50 mK.

The configuration of the ADR primarily reflects the need for the instrument to operate even in the case of a complete failure of the JT cooler or the complete loss of liquid helium. That is, while it would, for example, improve performance in cryogen-free mode to thermally and mechanically anchor Stage 2 to the JT cooler, a failure of the JT cooler would result in its temperature rising above 9 K, at which point Stage 2's NbTi magnet would be non-operational. The configuration therefore represents a compromise between thermodynamic efficiency[17] and the ability to achieve redundant operation.

The detector and ADR are assembled as an integral unit that is inserted into a well at the top of the helium tank, positioning the detector array at the focal point of a grazing-incidence x-ray mirror located at the top of the satellite. This arrangement minimized the number of thermal and mechanical interfaces to the dewar and JT cooler, and allowed performance and environmental testing on the completed assembly to be conducted at NASA/GSFC before delivery to Japan.

Assembly of the SXS instrument (detectors, ADR, helium tank, dewar and cryocoolers) was completed in mid-2014. Earlier this year (2015), all four science instruments (SXS, a Soft X-ray Imager [SXI], a Hard X-ray Imager [HXI] and a Soft Gamma ray Detector [SGD]) were integrated with the Astro-H spacecraft. This represented the most flight-like configuration in which the SXS instrument had yet been tested, and allowed compatibility with the other instruments and spacecraft systems to be probed. The satellite is currently being prepared for thermal vacuum testing and final vibration testing, after which the four grazing-incidence x-ray mirrors will be installed. The satellite will then be shipped to the launch site at Tanegashima Space Center, Japan, where it is scheduled to launch in late January 2016.

A significant portion of the testing time that was built into the development schedule was used for calibration of the detectors and to develop the control algorithms – primarily for cryogen-free mode – that are critical to the ADR meeting not only its minimum cooling requirements, but having enough margin to compensate for off-nominal conditions on orbit, such as degradation in cryocooler performance over time or elevated heat loads. This development has resulted in a robust cooling system that meets all of its requirements in both cryogen and cryogen-free operating modes, and that has also demonstrated the ability to begin detector operation when the detectors, ADR and helium tank are warmed up and cooled back down to 4.5 K by the JT cooler. This paper summarizes the operation and performance of the SXS ADR in these modes.

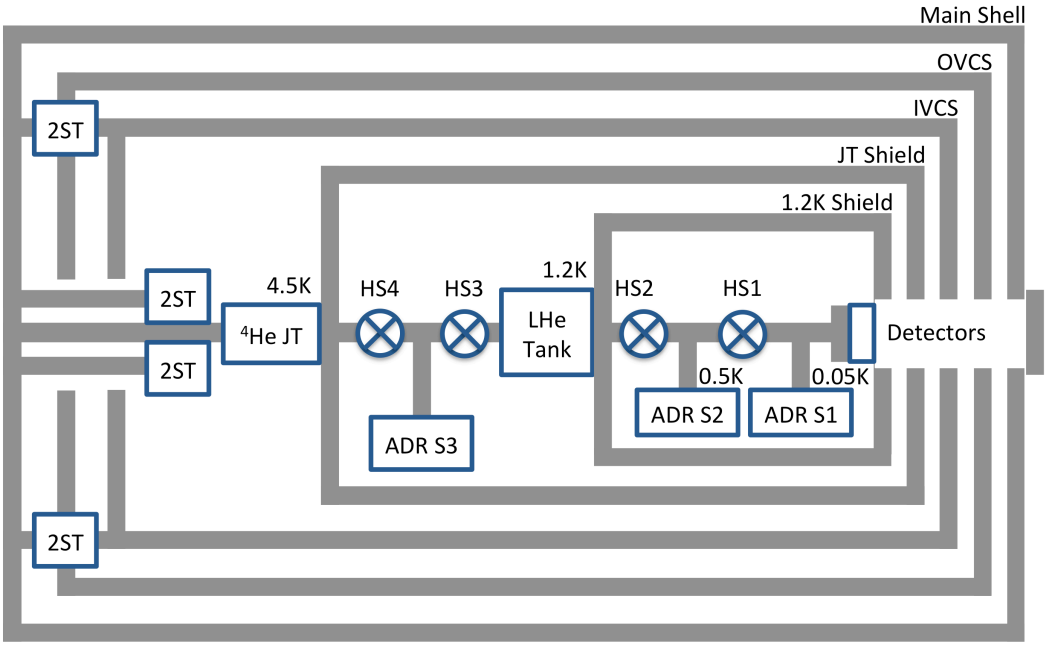

Figure 1. Schematic representation of the SXS cryogenic system. Four 2-stage Stirling cryocoolers (2ST) are used to cool the inner and outer vapor cooled shields (IVCS, OVCS) and precool the JT cooling loop.

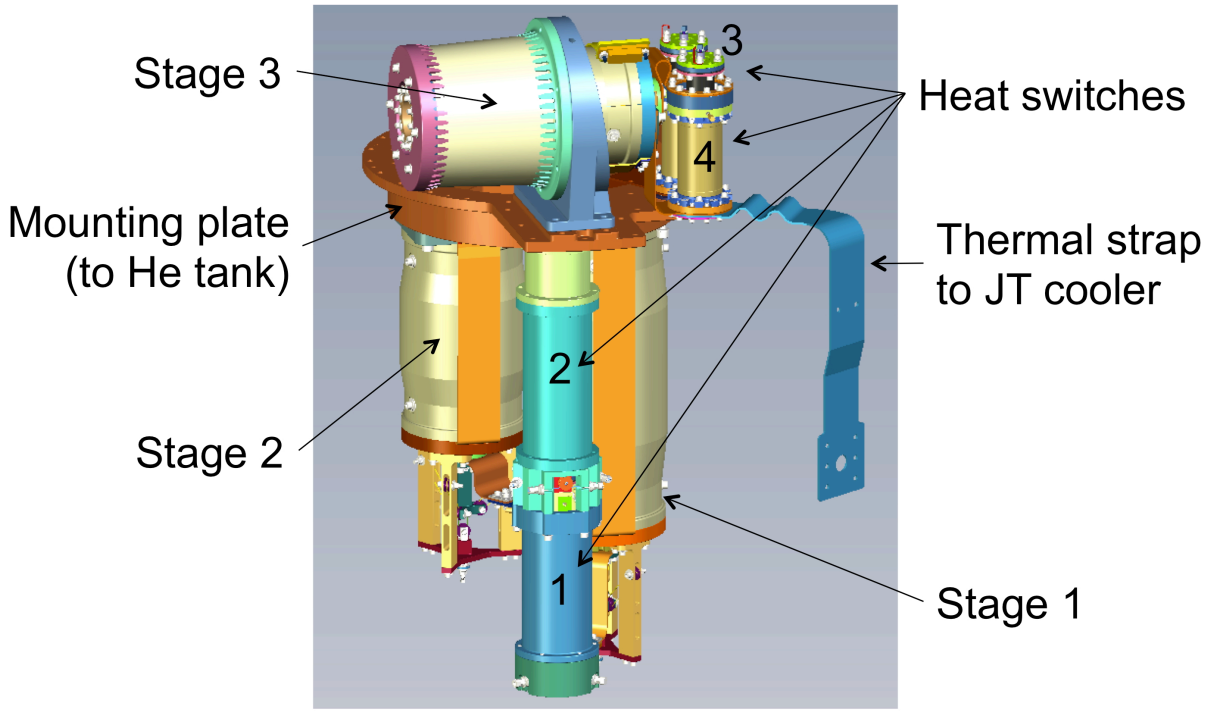

Figure 2. Solid model representation of the SXS ADR.

CRYOGEN MODE OF OPERATION

Recycling Sequence

Cooling the detectors in cryogen mode is accomplished using only Stages 1 and 2. While many recycling sequences can be used, the sequence implemented here compensates for the late addition of an electrical isolator in the thermal path between the Stage 1 salt pill and its heat switch. In earlier designs of the ADR, the heat switch itself provided electrical isolation, as its containment shell – composed of T300 composite and Ti15333 foil – was made to be non-electrically conductive[13]. Reliability concerns drove a change to all-metal (Ti15333) shells[18] and the need for an auxiliary means of isolating the detectors and salt pill from ground. Because of envelope constraints, the isolator had to be very small and capable of being integrated into the existing assembly. It consists of two 0.5 mm thick disks of gold-coated copper bonded together with a thin layer of Stycast 1266[19], and is inserted between the cold end of HS1 and the thermal strap that links it to the salt pill. Due to thermal boundary effects, the isolator significantly reduces the thermal conductance between Stages 1 and 2, especially below 1 K.

The recycling sequence was modified to allow the majority of heat to flow between the two stages at temperatures above 1 K. A secondary advantage is that the same control algorithm can be used regardless of starting temperatures and currents in the two stages. The control algorithms are implemented in a simple state machine in the ADR control (ADRC) electronics,

which exert control only through powering heat switches on and off, and regulating each stage's temperature via PID feedback loops (whose output is magnet voltage).

The recycling sequence involves first magnetizing both stages to a temperature 10% higher than that of the helium tank. When Stage 2 is warmer than the tank, HS2 is powered on; when Stage 1 is warmer than Stage 2, HS1 is powered on. In this state, both stages will reach their maximum currents (2 amps for both), HS2 is powered off and Stage 2 is regulated at a temperature 10% below that of Stage 1. By continuously updating Stage 2's setpoint, both stages steadily cool until Stage 1 reaches its target demagnetization temperature of 0.8 K. HS1 is then powered off and Stages 1 and 2 are demagnetized to 50 mK and 0.5 K, respectively. Stage 1's feedback loop bases its control on a germanium resistance thermometer directly coupled to the detector array.

Figure 3 depicts the recycling process when it is performed at the completion of a hold period. The time required for recycling from this condition is 44 minutes. When the cycle is started from a "warm" state, with both salt pills at ~1.2 K, the larger amount of heat that has to be rejected extends the recycle time to 60 minutes. In both cases, the detectors require about 20 minutes after reaching 50 mK to reach the stability level required for science operations.

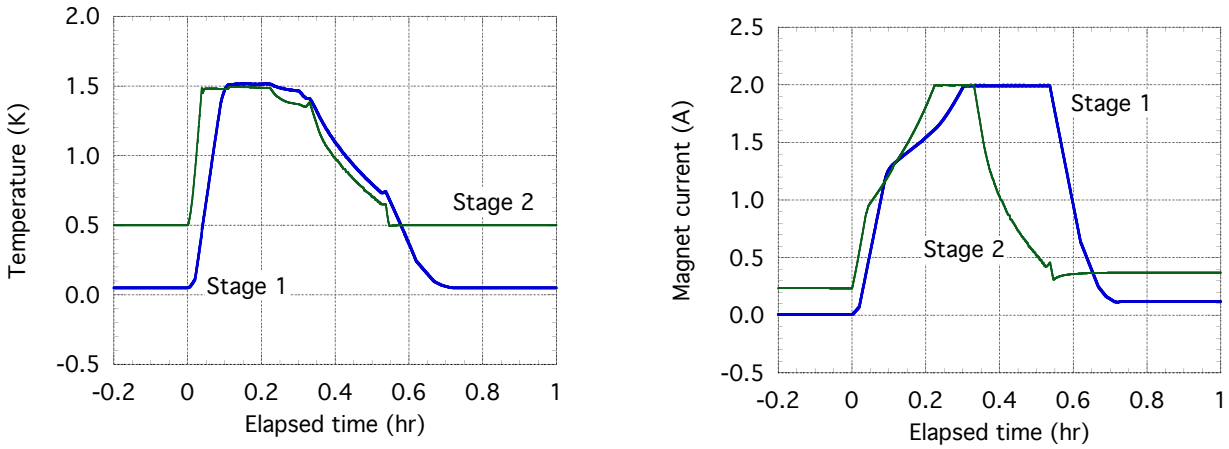

Figure 3. Temperatures and currents during a 2-stage ADR recycle following the completion of a hold period.

Figure 4 shows the repeating pattern of current and temperature in Stage 1 that results when the stage is automatically recycled when its magnet current falls below 5 mA. At this threshold, the remaining hold time of less than 0.5 hours is sacrificed in order to ensure that the detectors are always operating at the required temperature stability.

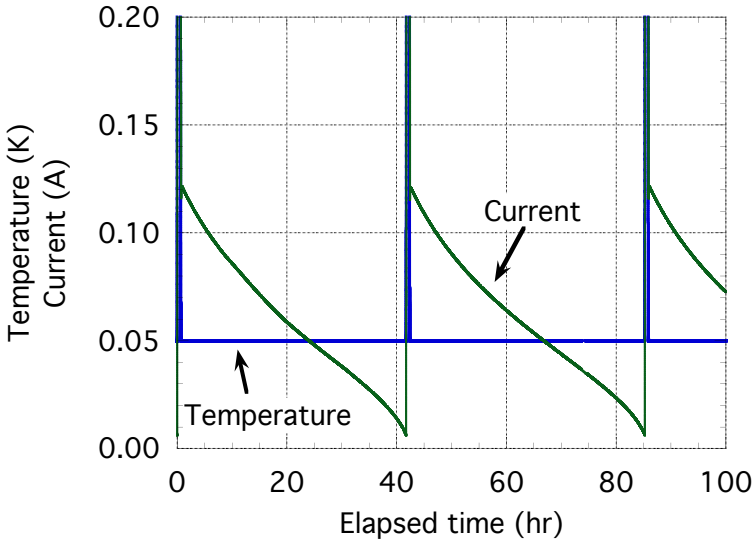

Figure 4. Stage 1 temperature and current during successive hold periods. Elapsed time is from the start of a recycle.

Heat Loads, Hold Time and Duty Cycle in Cryogen Mode

The theoretical cooling capacity of Stage 1, when demagnetized from a field of 2.0 T at 0.8 K, is 0.165 J. Integrating the measured heat load of 0.86 μW over the hold time gives a capacity of 0.132 J, which is 84% of the theoretical value. This percentage reflects certain expected inefficiencies in the ADR. First, due to the limited thermal conductance of strap that links the detector array to the salt pill, the salt must cool below 50 mK, reducing its entropy capacity and increasing the entropy usage rate. The salt temperature was determined to be 48.5 mK by fitting the current as a function of time (under constant heat load) to standard demagnetization curves[20]. Second, the average magnetic field in the region of the salt, 1.92 T, is less than the design goal of 2 T. Third, some of the salt pill's cooling capacity is used in cooling itself and the detector array to low temperature. Finally, there can also be eddy current losses and internal gradients within the salt pill during demagnetization that further reduce the available cooling capacity, though these are expected to be very small at the demagnetization rates used. Nevertheless, the actual cooling capacity is considerably larger than assumed (70% of the theoretical maximum) in the design phase.

The heat load to the cold stage has three main contributions: the detector heat load, conduction through HS1, and conduction through the Kevlar suspension systems that thermally link Stage 1 to the helium tank. Other loads, such as from sensor wiring, are negligible. As is typical for an ADR designed to survive launch[14], the Kevlar suspensions represent the majority of the heat load. Figure 5 shows the expected heat loads to 50 mK as a function of helium tank temperature. Table 3 lists the current best estimate for individual contributions with the helium tank at 1.20 K. The estimated total is 0.65 μW, whereas the measured load is 0.86 μW.

The discrepancy is not easily traced to an individual component, since only in the current assembly-level testing has the environment been stable enough to obtain definitive heat load measurements. That is, in all previous tests at various levels of assembly, extraneous heat loads – possibly due to thermal radiation and/or mechanical vibration from the commercial cryocooler – were observed that could not be separated from those originating in the flight hardware. This leaves the source of the discrepancy unresolved, though a likely candidate is the detector heat load, which was derived in part from unpublished thermal conductivity data for Kevlar 49. Adjusting the Kevlar contribution using more recent measurements [X[21]] yields almost exactly the measured heat load. These kinds of uncertainties, though, reinforce the wisdom of applying the 100% margin factor to estimated heat loads during the design phase.

The demonstrated hold time (as seen in Figure 4) exceeds 42 hours. Including the ~20-minute detector equilibration period, the time between science observations at 50 mK is just over 1 hour (64 minutes on average). The SXS instrument achieves a duty cycle in excess of 97%.

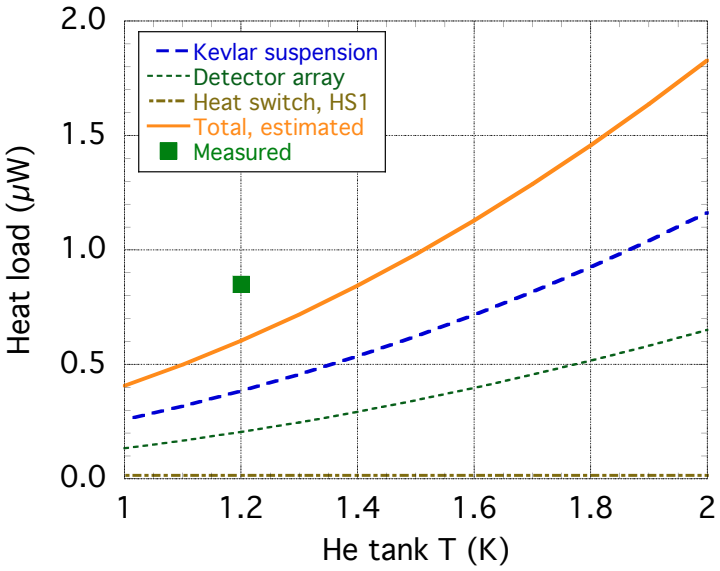

Figure 5. Heat loads to 50 mK as a function of helium tank temperature in cryogen mode. Note that the heat switch HS1 parasitic is constant, as it does not thermally connect to the tank.

Table 3. Estimated and measured heat loads in cryogen mode, when the He tank temperature is 1.20 K.

Heat source	*Heat load (μW)*
Detector array	0.25
Salt pill/heat switch suspension	0.38
Heat switch (HS1)	0.017
Estimate total	0.65
Measured total	0.86

Temperature Stability in Cryogen Mode

The temperatures of the detector array and the detector housing are shown in Figures 6a and 6b. These data were taken with all cryocoolers at nominal power, and vibration isolators installed between the dewar main shell and all four Stirling compressors. The standard deviation of the array temperature over this time interval is 0.54 μK rms, well within the requirement of 2 μK rms (see Table 1).

In the plot of detector housing temperature, obtained when the tank was approximately 30% full, the required stability period is identified with markers. At the beginning of that interval, the liquid helium is cooling after absorbing the approximately 15 J of heat rejected from the ADR. In this case, the maximum drift in detector housing temperature in any 10-minute period is 0.5 mK. Short-term fluctuations are far smaller. The initial rise in temperature and subsequent drift rates will increase as the liquid volume decreases, but the effective heat capacity of the liquid is high enough that the detector housing will remain stable, to within the 1 mK requirement, at all fill levels.

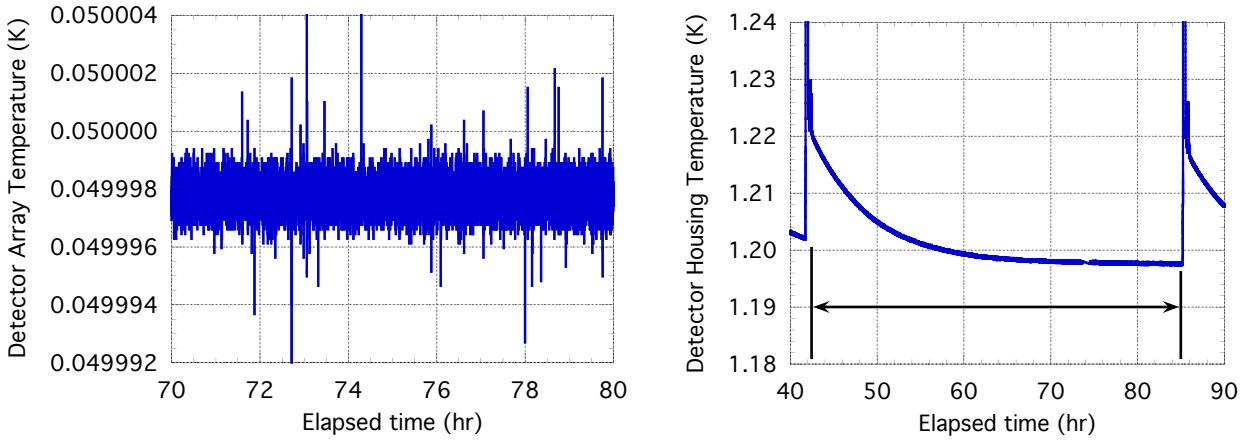

Figure 6. Temperature stability during cryogen mode operation of (left) the detector array at 50 mK and (right) the detector housing. Note that a small temperature offset is applied to the detector array control in order to match the conditions at which the detectors were calibrated.

CRYOGEN-FREE MODE OF OPERATION

The ADR's cycling sequences are fundamentally different in cryogen-free mode than in cryogen mode, driven by the need to meet the challenging stability criteria for the detector housing. When operation begins, HS2 is powered on continuously (except for the short time when Stage 1 is recycled) in order to thermally couple Stage 2 to the helium tank, and hence to the detector housing. Its PID loop is switched to use a thermometer on the detector housing as

its control input, rather than one on the salt pill, so that its primary function is to stabilize the housing temperature.

At the same time, Stage 3 begins continuous cycling to remove heat from the helium tank and reject it to the JT cooler. This cycling, shown in Figure 7, is a completely independent process that relies only on real time measurements of the tank and JT temperatures. Of course, the fact that Stage 2 is working to stabilize the tank temperature leads to an interaction in which heat flows between the two stages. The net effect is that Stages 2 and 3 work cooperatively to continuously cool the helium tank.

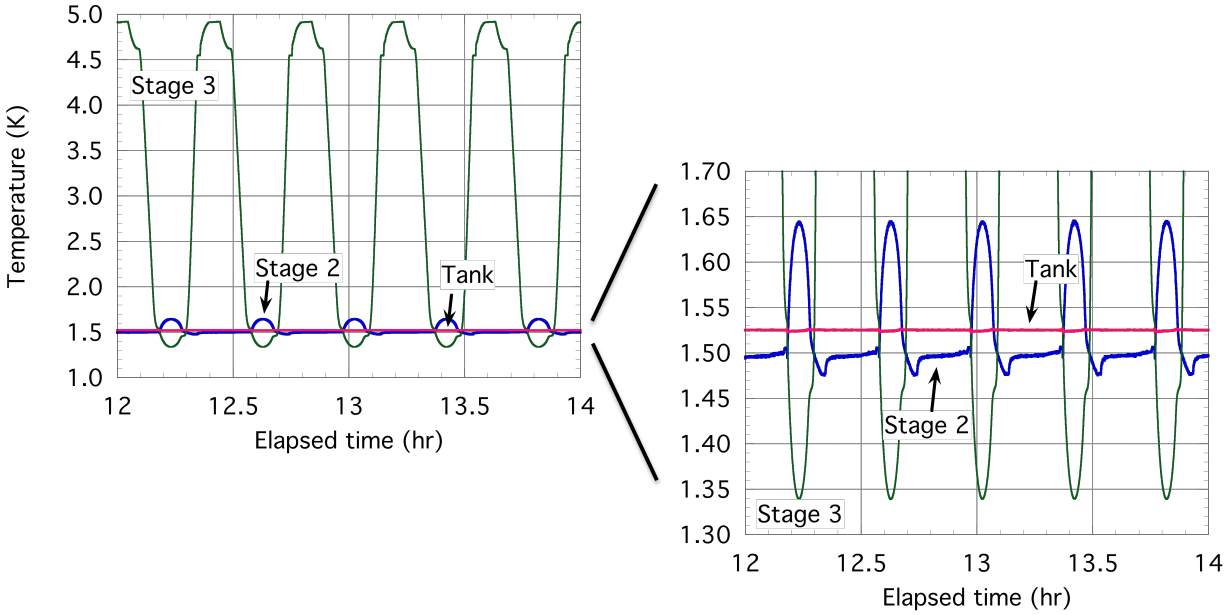

Figure 7. The combined operation of Stages 2 and 3 resulting in continuous cooling of the helium tank.

The temperature setpoint for Stage 2 is chosen so that Stage 3's cooling power, which is close to linear in tank temperature, exceeds the time average heat load on the tank. Stage 2 supplies the extra heat, leading to a gradual charging of its magnet, as seen in Figure 8. The rising magnetic field represents stored cooling capacity, which at currents above about 1.7 amps is enough to recycle Stage 1 at the end of its hold time. Stage 3's cooling is throttled to prevent Stage 2 from reaching its maximum current, at which point it would lose the ability to control temperature.

There are a number of competing factors that influence the choice of tank setpoint. A lower setpoint improves Stage 1's hold time, giving Stage 2 a longer time to build current. On the other hand, Stage 3's cooling power decreases with setpoint, slowing the rate at which Stage 2 builds current. A third consideration is that if Stage 2 builds current too early, the ohmic heating of its magnet leads increases the IVCS temperature, which increases the heat load on the JT cooler. The latter has the undesirable effect of reducing Stage 3's cycle speed and its cooling power, making it more difficult for Stage 2 to resume control of the tank after a recycle. Taken together, the goal is to select a setpoint that results in Stage 2 reaching maximum current just at

the end of Stage 1's hold time. For the cryogenic system as it is currently operated, in terms of cryocooler input powers and the ADR's control algorithms and PID parameters, the optimal setpoint is 1.525 K. As conditions change, the setpoint can be adjusted manually or allowed to adjust automatically, and the control electronics will immediately adapt.

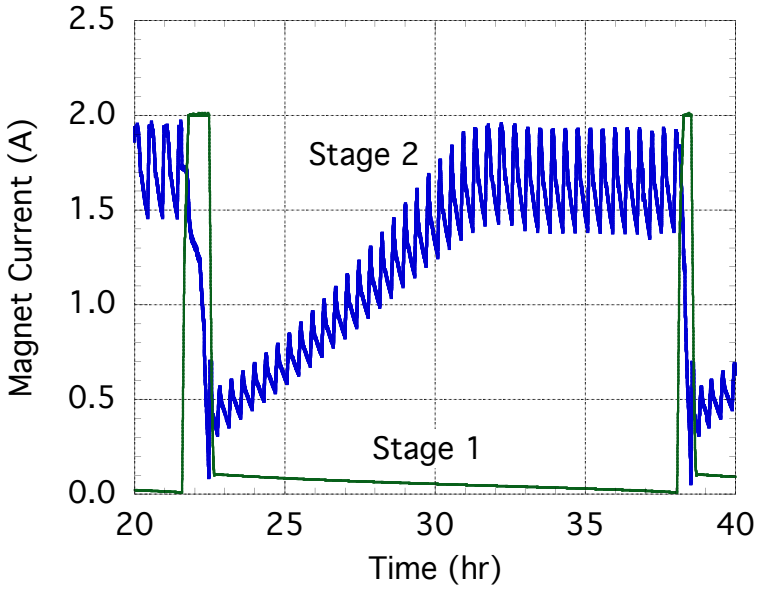

Figure 8. The progressive rise in Stage 2 current represents a buildup of cooling capacity needed to recycle Stage 1. The shorter-term sawtooth pattern results from Stage 2 alternating between net heat absorption and net heat rejection as Stage 3 cycles.

Figure 9 shows the stage temperatures when Stage 1 is recycled. The process is generally the same as for cryogen mode, except Stage 1 transfers heat only to Stage 2. HS2 is first powered off to decouple Stage 2 from the tank. Stage 1 is warmed above Stage 2 and HS1 is powered on. Stage 1 will automatically charge to full current, then Stage 2 precools it to 0.8 K. After powering off HS1, Stage 1 is demagnetized to 50 mK, and Stage 2 resumes control of the tank. The time needed to complete the recycle is 42 minutes.

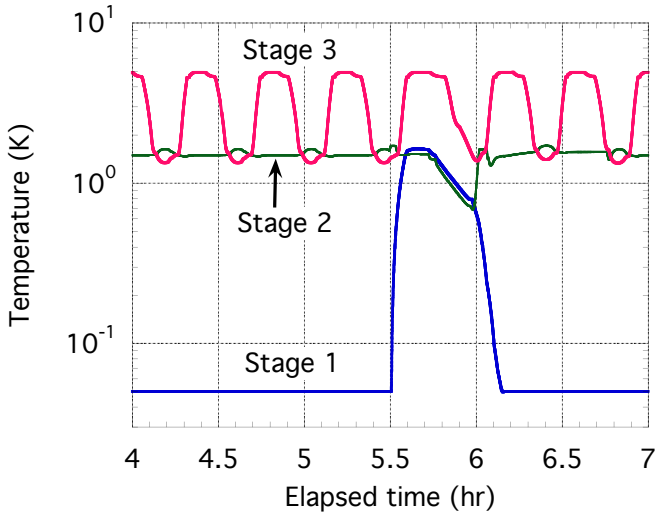

Figure 9. Temperatures of the three ADR stages during a cryogen-free mode recycle.

During the recycle the tank is not actively temperature controlled, but the cooling Stage 3 continues to generate maintains it near its setpoint. Stage 2 then resumes control with only modest loss of cooling capacity, mainly from its own hysteresis heat.

Stage 1 Heat Loads, Hold Time and Duty Cycle in Cryogen-Free Mode

The heat load on Stage 1 in cryogen-free mode is significantly larger than in cryogen mode, as both boundary temperatures that dictate the heat loads – the helium tank and Stage 2 – are warmer. Table 4 lists the individual and total estimated heat loads when the tank is regulated at 1.525 K, compared to the measured value. Figure 10 shows the dependence of these loads on tank temperature. As before, the discrepancy in heat loads is possibly explained by inaccurate material properties used in detector heat load estimate.

Table 4. Estimated and measured heat loads in cryogen-free mode, when the He tank is regulated at 1.525 K.

Heat source	*Heat load (μW)*
Detector array	0.36
Salt pill/heat switch suspension	0.62
Heat switch (HS1)	0.83
Estimate total	1.81
Measured total	2.29

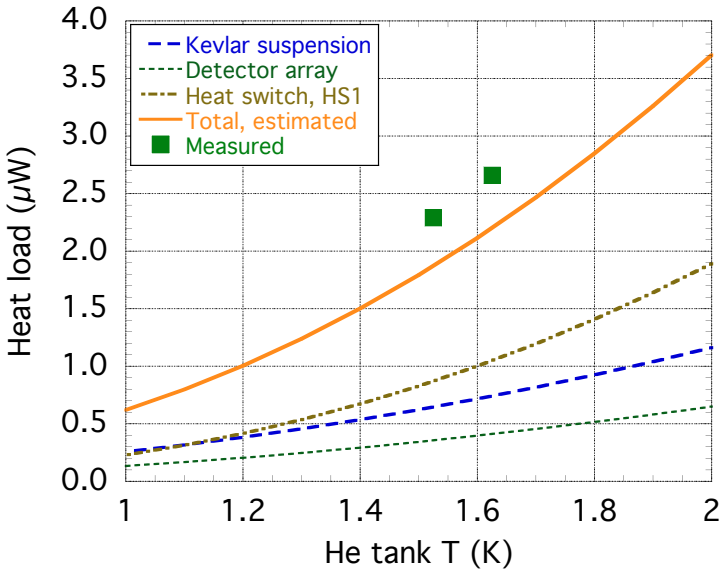

Figure 10. Heat loads to 50 mK as a function of helium tank temperature in cryogen-free mode.

Because Stage 1 is demagnetized from the same field and temperature as in cryogen mode, its theoretical cooling capacity remains 0.165 J. The measured hold time of 15.1 hours yields an integrated heat absorption of 0.124 J, or 75% of the theoretical maximum. Compared to cryogen mode operation, a lower percentage was expected, as the higher combined heat load results in a lower salt temperature, lower cooling capacity, and less efficient heat absorption.

The detector equilibration time after reaching 50 mK remains about 20 minutes, enabling science operations for 14.7 hours out of every 15.8 hours (hold plus recycle time). This translates to an observing efficiency of 93%, exceeding the requirement with margin.

Temperature Stability in Cryogen-Free Mode

A representative sample of detector array and detector housing temperatures are shown in Figure 11. The detector stability over extended periods is 0.63 μK rms, slightly worse than in cryogen mode, but still well within the requirement. A small contribution to the noise is synchronous with Stage 3 cycling, and results from Stage 2's temperature oscillation (seen in Figure 5) which produces a change in heat flow through HS1.

The detector housing exhibits excellent long-term stability, but there are short-term fluctuations as large as 3-4 mK on time scales of 10-15 seconds. These occur as Stage 2 transitions from net heat absorption to net heat rejection and vice versa. Although they exceed the 1 mK per 10 minute requirement, the detector response is not noticeably affected by them, so the requirement has been waived.

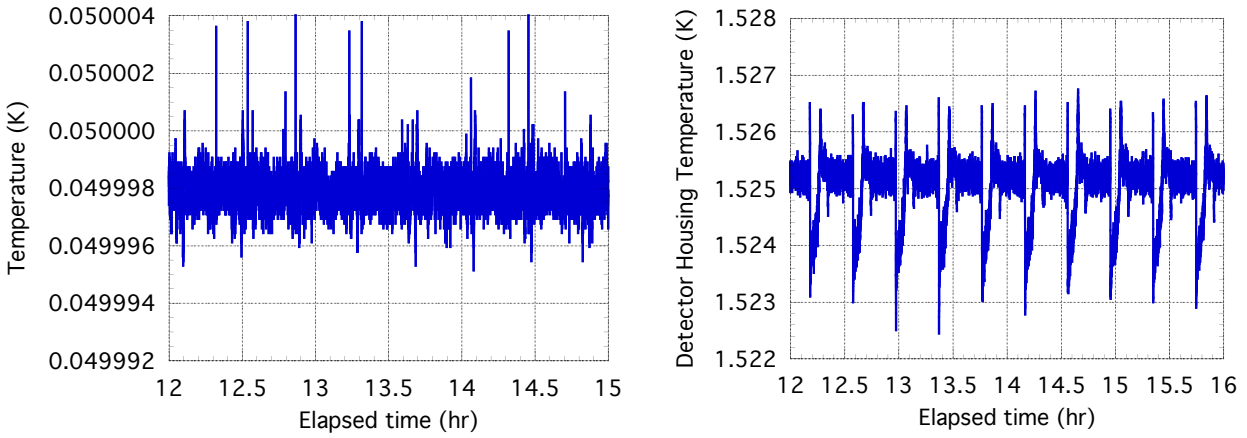

Figure 11. Temperature stability during cryogen-free operation of (left) the detector array at 50 mK and (right) the detector housing.

Warm Start from 4.5 K

While the transition from cryogen to cryogen-free mode on orbit likely will not involve any significant warming of the helium tank, there are situations in which it will be necessary for the ADR to begin operating with the detectors, ADR and helium tank all at the JT cooler's base temperature of 4.5 K. The ADR controller can accomplish the cooldown using the same algorithm used in normal operation since the algorithm was structured to adjust to a wide range of off-nominal conditions.

To begin, Stage 3 starts continuous cycling. With Stage 2 depleted of current, it is set to regulate the helium tank at an elevated temperature (2.5 K). However, the setpoint is well below the starting temperature, so the cooling produced by each cycle of Stage 3 goes into cooling the entire assembly, as seen in Figure 12. Once the tank is cooled below 2.5 K, Stage 2 begins building cooling (and entropy) capacity. Figure 12 also shows the entropy capacity of Stages 1 and 2 during the cooldown, referenced to the zero field entropy at their operating temperatures of 50 mK and 1.525 K, respectively. Positive entropy capacity equates to an ability of each stage to cool to those temperatures.

When Stage 2 reaches a threshold in entropy capacity, it begins to recycle Stage 1 as described previously. In this case, though, Stage 1 starts out depleted and the stored capacity in Stage 2 is insufficient to complete the recycle. After Stage 1 is charged as much as possible, it is stationed at an intermediate temperature while Stage 2 resumes building entropy capacity. When the threshold is again reached, Stage 1 is fully charged and precooled to its nominal demagnetization point. By this point, the ADR is in the same state as it would be under normal operating conditions, and the stages begin active control of the detectors and tank at 50 mK and 1.525 K. The time required to complete the cooldown is less than 7 hours.

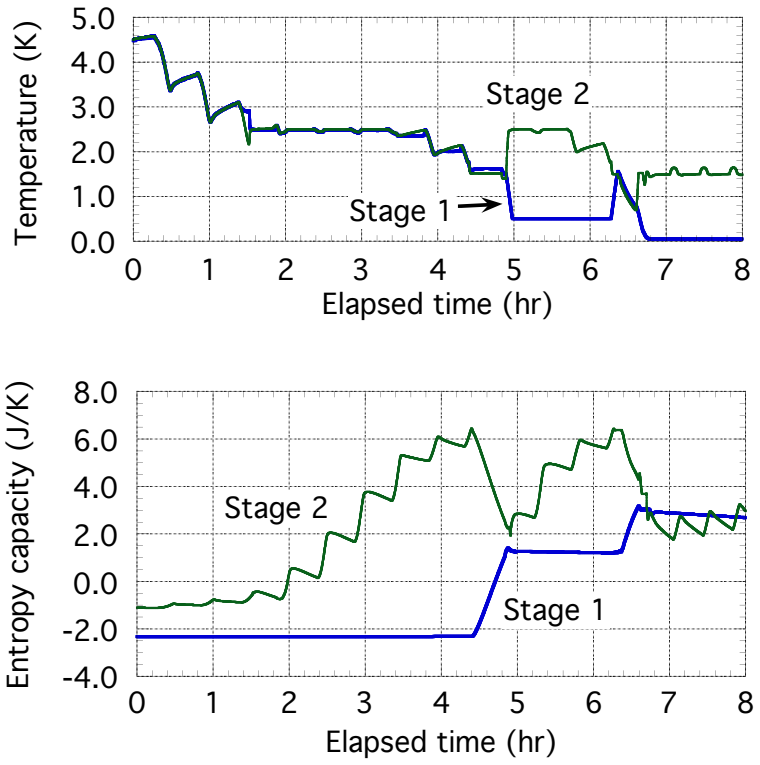

Figure 12. Stage 1 and 2 temperatures (top) and entropy capacities (bottom) during the cooldown from 4.5 K.

SUMMARY

NASA/GSFC has developed a detector assembly for the SXS instrument on Astro-H that uses a 3-stage ADR to cool a small 6x6 array of x-ray microcalorimeters to 50 mK. The ADR is configured to use either a superfluid helium tank (at ~1.2 K) or a 4.5 K JT cryocooler as a heat sink. The detector assembly was integrated into the flight dewar at Sumitomo Heavy Industries, Inc. in Japan in early 2014, and the SXS instrument has recently been installed on the Astro-H spacecraft for performance and compatibility testing. In the integrated system, the ADR has demonstrated the following cooling capabilities.

When operating with liquid helium at 1.20 K, the detectors are cooled by only two of the ADR's three stages. The CPA stage can hold them at 50 mK with a stability of typically 0.5-0.6 μK rms, for hold times of greater than 42 hours. Recycling takes about 45 minutes, after which the detectors require a ~20 minute stabilization period before science operations can resume. These durations yield a duty cycle of better than 97%. The heat load to 50 mK from both detector and parasitic sources is 0.86 μW, larger than the current best estimate of 0.65 μW based on as-built component dimensions and materials, plus the presumed detector heat load.

When the liquid helium is depleted on orbit, all three ADR stages will be used to cool the detectors to 50 mK and to continuously cool the helium tank to 1.525 K – a temperature chosen

so that the ADR generates enough excess cooling power to be able to recycle the CPA stage when needed. The heat load on that stage is higher – 2.29 μW – yielding a shorter hold time of just over 15 hours. The recycle and detector equilibration times are about 42 and 20 minutes, giving a duty cycle of better than 93%. The detector temperature stability is only slightly degraded from the cryogen mode case – 0.6-0.7 μK rms – while the detector housing much more stable over long time scales, but less stable on short ones. Nevertheless, detector performance is essentially the same in the two ADR modes.

The x-ray detectors are required to have better than 7 eV resolution for 6 keV x-rays. Early compatibility tests conducted with an engineering model of the instrument showed significant interference from cryocooler compressor vibration. With the installation of vibration isolators on all four Stirling compressors, the interference has been eliminated, and the detectors are consistently achieving 4.3 eV, very close to their intrinsic capability.

The Astro-H satellite is currently undergoing thermal vacuum tests, and will follow that with final vibration testing. The satellite will then be shipped to Tanegashima Space Center, Japan, for scheduled launch in late January 2016.

ACKNOWLEDGMENTS

This work was supported by NASA's Office of Space Science.

REFERENCES

[1] Shirron P, et al., "Design and Predicted Performance of the 3-Stage ADR for the Soft-X-Ray Spectrometer Instrument on Astro-H." *Cryogenics* 52 (2012):165-171.
[2] Mitsuda, K, *et al.*, 2010, "The high-resolution x-ray microcalorimeter spectrometer system for the SXS on ASTRO-H", Proc. SPIE 7732, Space Telescopes and Instrumentation 2010: Ultraviolet to Gamma Ray, pp. 773211-773211-10.
[3] Takahashi, T, *et al.*, 2010, "The ASTRO-H Mission", Proc. SPIE 7732, Space Telescopes and Instrumentation 2010: Ultraviolet to Gamma Ray, pp. 77320Z-77320Z-18.
[4] Ryuichi Fujimoto, et al., Cooling system for the soft X-ray spectrometer onboard Astro-H, *Cryogenics*, Volume 50, Issue 9, September 2010, Pages 488-493
[5] Mitsuda, K, et al., The High-Resolution X-Ray Microcalorimeter Spectrometer, SXS, on Astro-H, *J Low Temp Phys,*
[6] Kelley RL, et al., The Astro-E High Resolution X-Ray Spectrometer, Proceedings of SPIE
[7] Kelley RL, et al., The Suzaku High Resolution X-Ray Spectrometer, Publ. Astron. Soc. Japan 59, S77–S112, 2007 January 25
[8] Sato Y, et al., Development of mechanical cryocoolers for Astro-H/SXS, *Cryogenics*
[9] Yoshida S, et al., Flight model performance test results of a helium dewar for the soft X–ray spectrometer onboard ASTRO-H, *Cryogenics*, submitted for publication in this issue
[10] Peter J. Shirron, Mark O. Kimball, Bryan L. James, Donald C. Wegel, Raul M. Martinez, Richard L. Faulkner, Larry Neubauer, Marcelino Sansebastian, Design and predicted

performance of the 3-stage ADR for the Soft-X-ray Spectrometer instrument on Astro-H, *Cryogenics*, Volume 52, Issues 4–6, April–June 2012, Pages 165-171

[11] Peter J. Shirron, Dan McCammon, Salt pill design and fabrication for adiabatic demagnetization refrigerators, *Cryogenics*, Volume 62, July–August 2014, Pages 163-171

[12] Peter Shirron, Optimization strategies for single-stage, multi-stage and continuous ADRs, Cryogenics, Volume 62, July–August 2014, Pages 140-149

[13] Kimball M, Shirron P. Heat Switches Providing Low-Activation Power and Quick-Switching Time For Use In Cryogenic Multi-Stage Refrigerators. In: Advances In Cryogenic Engineering, Vols 57A AND 57B. Joint Conference on Transactions of the Cryogenic Engineering Conference (CEC)/International Cryogenic Materials Conference (ICMC); JUN 13-17, 2011; Spokane, WA. 2012. p. 853-858

[14] Bryan L. James, Raul M. Martinez, Peter Shirron, Jim Tuttle, John J. Francis, Marcelino San Sebastian, Donald C. Wegel, Nicholas M. Galassi, Daniel S. McGuinness, David Puckett, Yury Flom, Mechanical design of a 3-stage ADR for the Astro-H mission, Cryogenics, Volume 52, Issues 4–6, April–June 2012, Pages 172-177

[15] Numazawa T, Kamiya K, Shirron PJ, DiPirro MJ, Matsumoto K, "Magnetocaloric Effect of Polycrystal $GdLiF_4$ for Adiabatic Demagnetization Refrigeration", *AIP Conference Proceedings,* 850 (2006) 1579-1580.

[16] Patrick Wikus, Edgar Canavan, Sarah Trowbridge Heine, Koichi Matsumoto, and Takenori Numazawa, Magnetocaloric materials and the optimization of cooling power density, *Cryogenics* Volume 62, p. 150-162 (2014).

[17] Peter Shirron, Mark Kimball, Theo Muench, Michael DiPirro, Thomas Bialas, Gary Sneiderman, Scott Porter and Richard Kelley, Thermodynamic Performance of the 3-Stage ADR for the Astro-H Soft-X-ray Spectrometer Instrument, *Cryogenics,* submitted for publication in this issue.

[18] Kimball MO and Shirron PJ, Fast-response, active gas-gap heat switches for low temperature applications, submitted for publication in the proceedings of the 2015 Cryogenics Engineering Conference, Tucson AZ (2015).

[19] Stycast 1266 is a product of Emerson-Cummings

[20] Peter J. Shirron, Applications of the magnetocaloric effect in single-stage, multi-stage and continuous adiabatic demagnetization refrigerators, *Cryogenics*, Volume 62, July–August 2014, Pages 130-139

[21] Ventura G, Barucci M, Gottardi E, and Peroni I, Low temperature thermal conductivity of Kevlar, *Cryogenics* 40 (2000) 489-491.